

1 **ROBUST METABOLOMICS APPROACH FOR THE EVALUATION OF HUMAN EMBRYOS**  
2 **FROM IN-VITRO FERTILIZATION**  
3  
4 **Cecilia Beatriz Figoli, Marcelo Garcea, Claudio Bisioli, Valeria Tafintseva, Volha**  
5 **Shapaval, Mariana Gómez Peña, Luz Gibbons, Fernando Althabe, Osvaldo**  
6 **Miguel Yantorno, Marcos Horton, Jürgen Schmitt, Peter Lasch, Achim Kohler\***  
7 **& Alejandra Bosch\***  
8

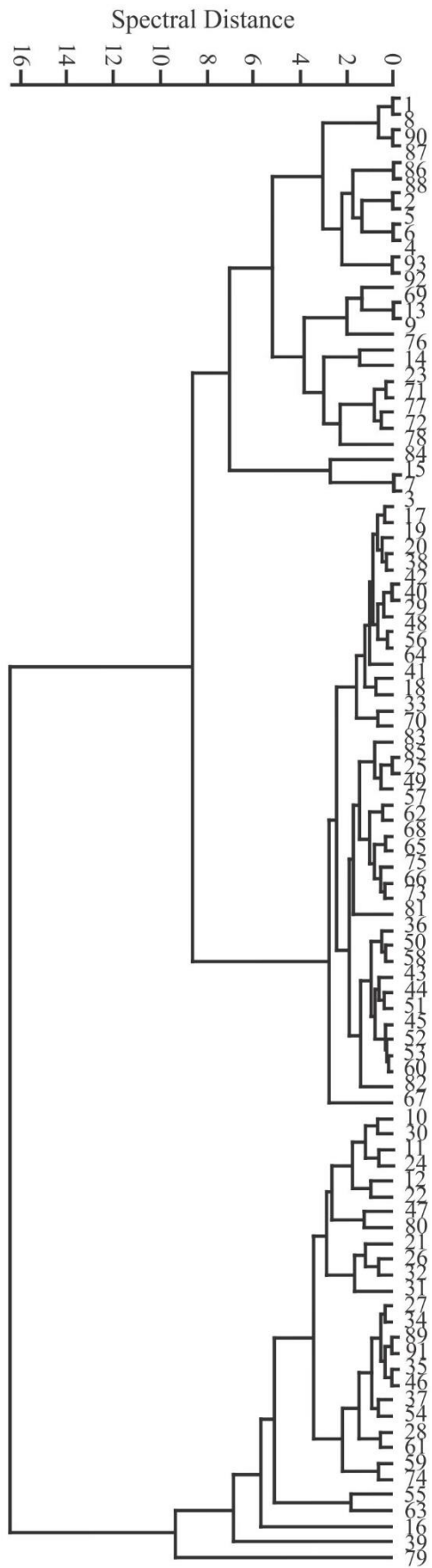
9 \*Corresponding author:  
10 Alejandra Bosch, E-mail: [bosch@quimica.unlp.edu.ar](mailto:bosch@quimica.unlp.edu.ar)  
11 Achim Kohler, E-mail: [achim.kohler@nmbu.no](mailto:achim.kohler@nmbu.no)  
12

13 **SUPPLEMENTARY INFORMATION INCLUDES:**  
14 **SUPPLEMENTARY NOTE 1**  
15 **SUPPLEMENTARY FIGURES 1 TO 8**  
16

17 **Supplementary Note 1: Heterogeneity analysis of IMP and NIMP spectra.** The  
18 unsupervised hierarchical-cluster-analysis was used for the evaluation of the  
19 heterogeneity of IMP and NIMP. As previously reported<sup>46</sup> and detailed in the  
20 Materials and Methods section, the spectral variances in each data set were  
21 determined as the average  $\pm$  2 standard deviations of the so-called spectral distance  
22 ( $D$ )<sup>52,66,67</sup>. This parameter corresponds to a dissimilarity measurement equal to  $(1 - r)$   
23  $\times 1000$ , with  $r$  being Pearson's product-moment–correlation coefficient. The spectral  
24 distances were calculated through the use of the preprocessed procedure  $B$  in the  
25 spectral ranges 1500–1800  $\text{cm}^{-1}$  and 730–1280  $\text{cm}^{-1}$ . The fusion values in

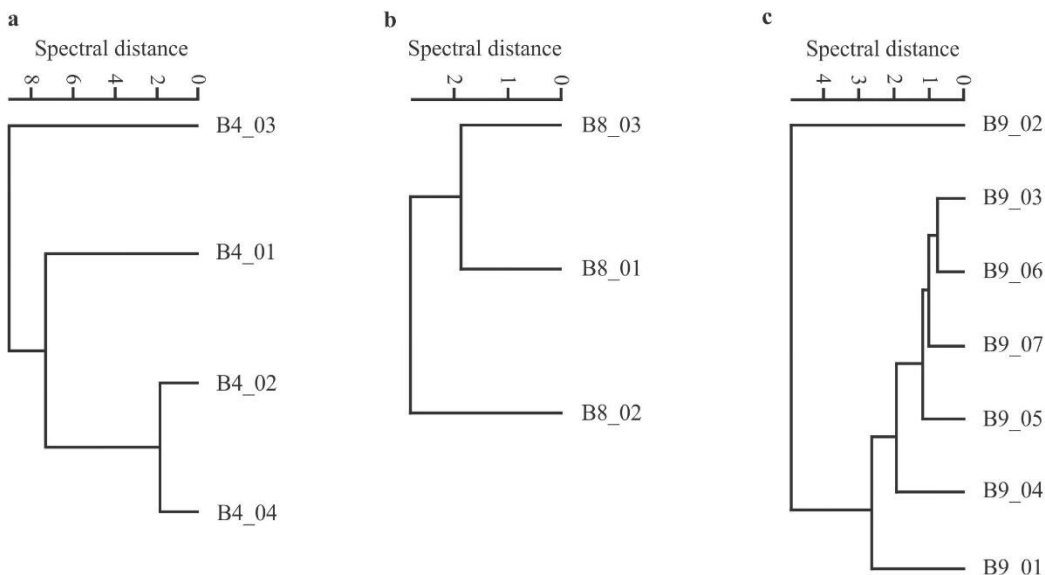
26 dendrograms were obtained by means of the average linkage (OPUS versions 7.0  
27 Bruker Optics GmbH, Ettlingen, Germany).

28 The heterogeneity obtained for IMP ( $D \pm SD = 11.70 \pm 7.00$ ) was smaller than  
29 that obtained for NIMP ( $D \pm SD = 21.98 \pm 16.97$ ). This analysis indicated that IMP  
30 spectra were quite homogenous, while those from NIMP were highly heterogeneous  
31 (Supplementary Fig. 4). These results support the analysis of the spectral-data internal  
32 structure performed by principal-component analysis.



34 **Supplementary Fig. 1 Reproducibility levels of acquired spectra among the**  
35 **different wells in the ZnSe optical plate.** The spectral distances were calculated  
36 through the use of the preprocessed procedure A in the spectral ranges 3000–2800 cm<sup>−1</sup>,  
37 1800–1550 cm<sup>−1</sup>, 1500–1250 cm<sup>−1</sup>, and 1200–900 cm<sup>−1</sup>. The fusion values in  
38 dendograms were obtained by means of the average linkage (OPUS software 7.0,  
39 Bruker, Optics, Germany). The spectral distance measured for this independent  
40 replicate was  $6.30 \pm 5.26$ . The analysis indicated that the spectral quality was not  
41 affected by the sample desiccation that occurred during the time period required for  
42 the measurements. Three wells of the ZnSe microtiter plate remained empty. One well  
43 (A1) was used to measure the spectrum background and the other position were  
44 measured empty in order to stabilize the air circulation of the equipment.

45

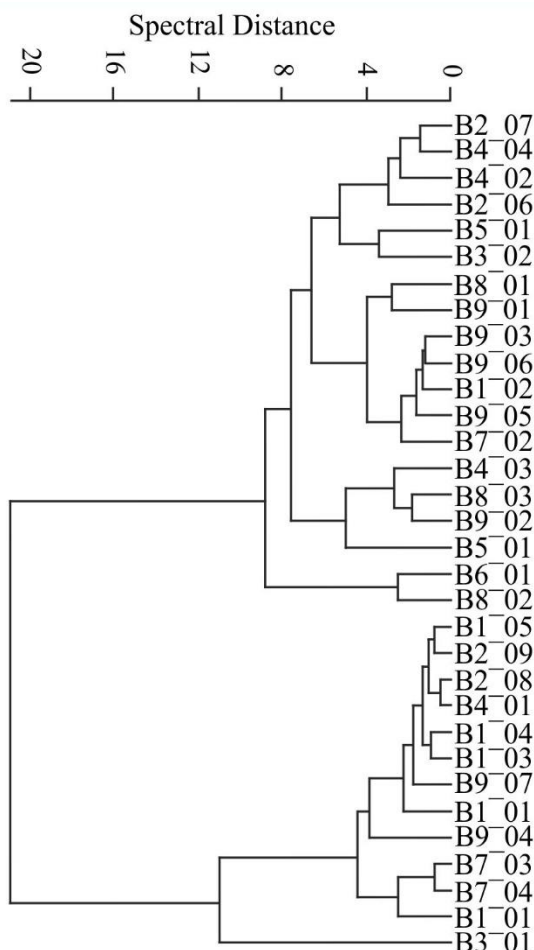


46  
47 **Supplementary Fig. 2 Reproducibility among each batch of culture medium G1**  
48 **Plus.** Reproducibility levels among three different batches of G1 Plus culture  
49 medium. Panel a, Batch 4; Panel b, Batch 8; Panel c, Batch 9. The spectral distances  
50 were calculated through the use of the preprocessed procedure A in the spectral ranges

51 3000–2800 cm<sup>−1</sup>, 1800 cm<sup>−1</sup>, 550 cm<sup>−1</sup>, 1500–1250 cm<sup>−1</sup>, and 1200–900 cm<sup>−1</sup>. The  
52 fusion values in dendograms were obtained by means of the average linkage (OPUS  
53 software 7.0, Bruker, Optics, Germany). The widest spectral distances measured for  
54 these culture-medium batches were  $7.08 \pm 3.29$  (Panel a),  $2.50 \pm 0.94$  (Panel b) y  $3.34$   
55  $\pm 2.53$  (Panel c), respectively. The reproducibility obtained within each batch of G1  
56 Plus culture medium exhibited a low level of variability.

57 B: batch

58



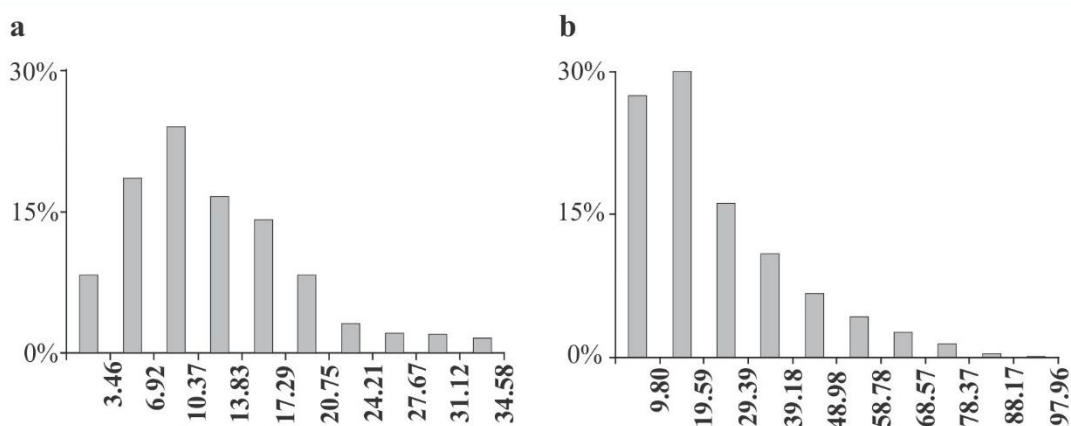
59

60 **Supplementary Fig. 3 Reproducibility among batches of culture medium G1**  
61 **Plus.** The spectral distances were calculated through the use of the preprocessed  
62 procedure A in the spectral ranges 3000–2800 cm<sup>−1</sup>; 1800–1550 cm<sup>−1</sup>; 1500–1250 cm<sup>−1</sup>,  
63 and 1200–900 cm<sup>−1</sup>. The fusion values in dendograms were obtained by means of

64 the average linkage (OPUS software 7.0, Bruker, Optics, Germany). The widest  
65 spectral distance measured for analysis of the variance of these G1 Plus culture  
66 medium batches was  $9.31 \pm 6.60$ . This analysis indicated that a high level of  
67 reproducibility was observed, while no significant spectral differences were recorded  
68 for more than 15 different batches of G1 Plus culture medium assayed.

69 B: batches

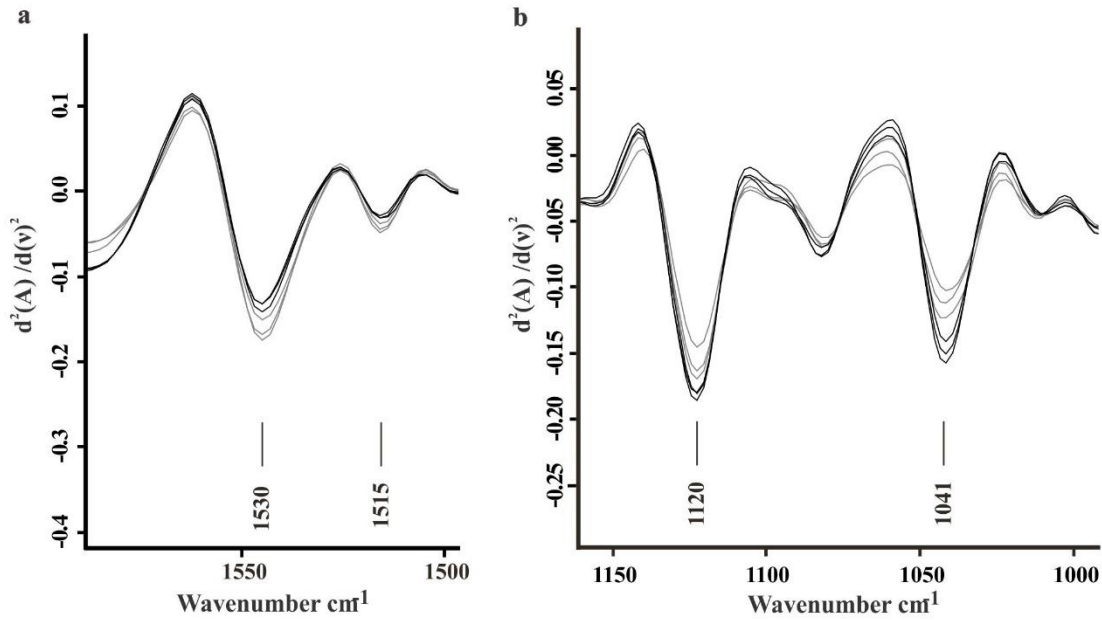
70



71

72 **Supplementary Fig. 4 Heterogeneity of the spectra within classes.** Distribution of  
73 spectral-distance values of spectra acquired from 3-day-embryo supernatants  
74 belonging to IMP (Panel a) and NIMP (Panel b). In the two panels, the percent  
75 distribution of each spectral distance indicated on the *abscissa* is plotted on the  
76 *ordinate*.

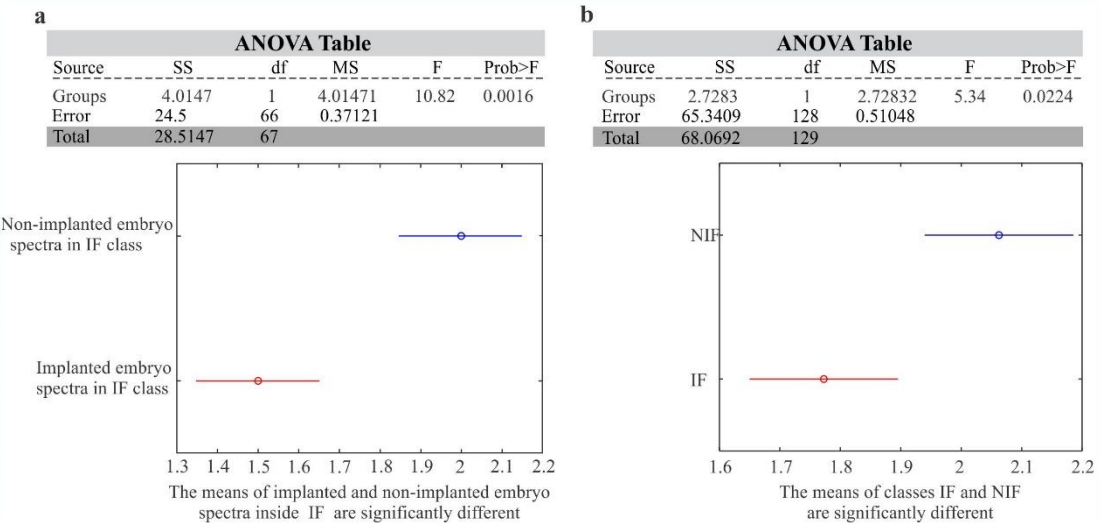
77



78

79 **Supplementary Fig. 5 Spectral differences in the regions W2 and W4.** In both  
80 panels of the figure, the second derivative of the spectra is plotted on the *ordinate* as a  
81 function of the wavenumber on the *abscissa*. Panel a: Vector-normalized second-  
82 derivatives of the three spectra of the IF (black line) and NIF (gray line) classes at  
83  $1530\text{ cm}^{-1}$  associated with amino acids. Panel b: Vector-normalized second-  
84 derivatives of the three spectra of the IF (black line) and NIF (gray line) classes at  
85  $1120\text{ cm}^{-1}$  and  $1041\text{ cm}^{-1}$  assigned to the C–O stretching in the carboxylic group of  
86 lactate.

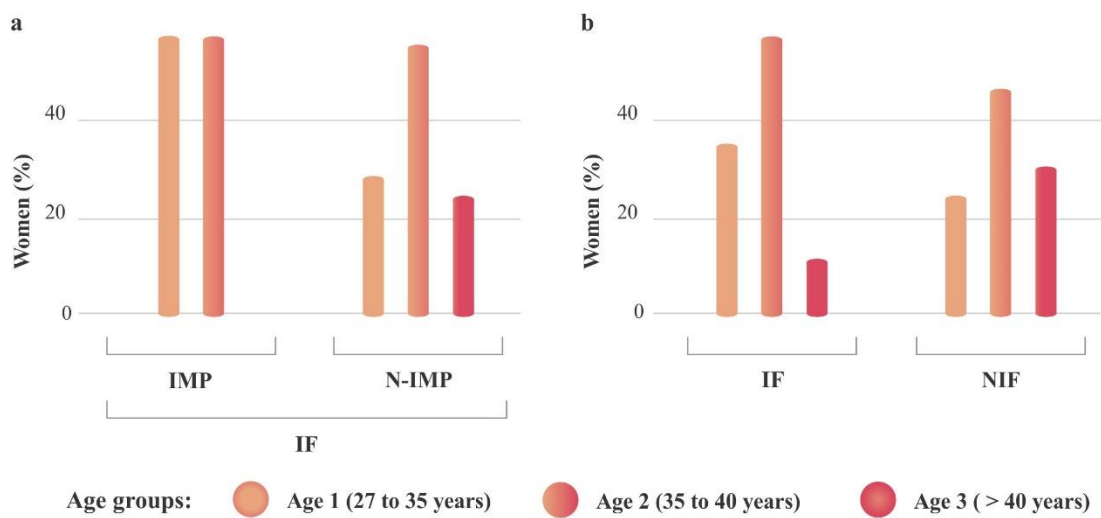
87



88

89 **Supplementary Fig. 6** Panel a: One-way ANOVA evaluating maternal age in the IF  
90 class ( $p < 0.05$ ). The statistical analysis demonstrated that within this IF class the age  
91 of the mothers was significantly different between the class-IMP- and the class-  
92 NIMP-embryo spectra, with the mothers being older in class NIMP. Panel b: One-  
93 way ANOVA comparing maternal ages and metabolomic-fingerprint classes ( $p$   
94  $< 0.05$ ). The analysis indicated that the embryo-supernatant samples classified as NIF  
95 were from older mothers than those classified as IF.

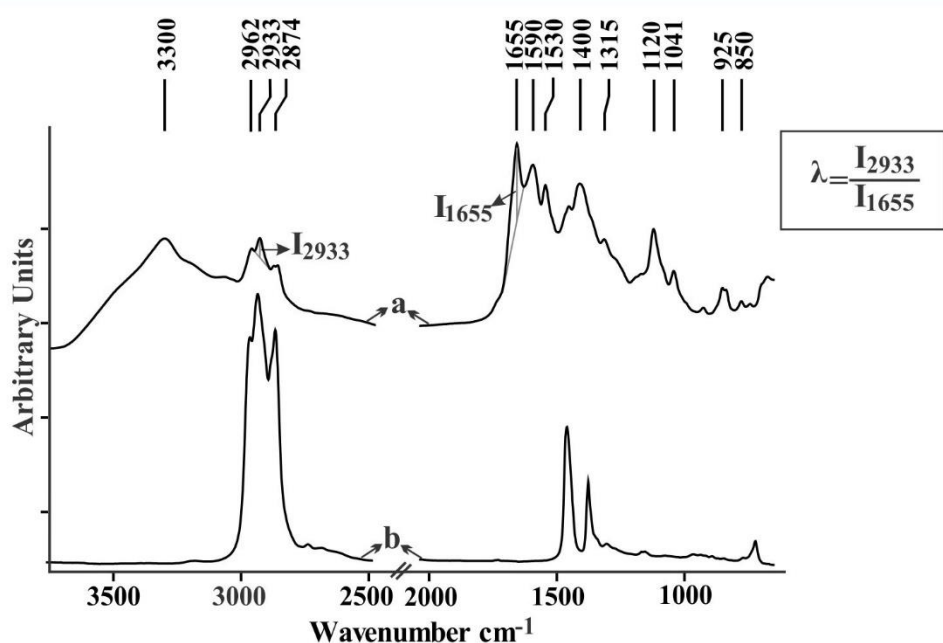
96



97

98 **Supplementary Fig. 7 Analysis of the age percentage distribution of women**  
99 **considering the defined age categories.** Panel a: Maternal-age analysis between

100 samples from implanted embryos (IMP) and nonimplanted embryos (NIMP) of the IF  
101 class. Panel b: Maternal-age analysis between samples from the IF and NIF classes. In  
102 the two panels, the percent of the women within a given age class is plotted on the  
103 *ordinate* with respect to the transferred embryos having the implantation outcomes.  
104 Age Groups: Age 1 (27 to 35 years), Age 2 (35 to 40 years), Age 3 (>40 years).  
105



106  
107 **Supplementary Fig. 8 Determination of oil contamination in 3-day-embryo–**  
108 **supernatant spectra.** In the figure, the absorbance in arbitrary units is plotted on the  
109 *ordinate* as a function of the wavenumbers indicated in the *abscissa*. Spectrum a:  
110 FTIR spectrum of a 3-day-embryo supernatant contaminated with culture oil.  
111 Spectrum b: FTIR average spectrum of the oil. The intensity of the  $-\text{CH}_2$  stretching of  
112 lipids at  $2933 \text{ cm}^{-1}$ —used as a marker band for the oil content—and the amide-I band  
113 at  $1655 \text{ cm}^{-1}$ —an internal standard for the total material—can be used to determine  
114 the relative amount of oil present in the spectra of embryo supernatants.